JOURNAL OF BACTERIOLOGY, Mar. 1997, p. 1846–1851 Vol. 179, No. 6
0021-9193/97/$04.00+0

Isolation and Characterization of a Molecular Chaperone, gp57A, of Bacteriophage T4

TAKURO MATSUI,[1] BRONYA GRINIUVIENÉ,[2] EDWARD GOLDBERG,[2] AKIRA TSUGITA,[3] NOBUO TANAKA,[1] AND FUMIO ARISAKA[1]*

Department of Life Science, Faculty of Bioscience and Biotechnology, Tokyo Institute of Technology, 4259 Nagatsuta, Midoriku, Yokohama 226,[1] and Research Institute for Biosciences, Science University of Tokyo, Yamazaki Noda 278,[3] Japan, and Department of Molecular Biology and Microbiology, Tufts University Medical School, Boston, Massachusetts 02111[2]

Received 8 July 1996/Accepted 3 January 1997

A molecular chaperone of bacteriophage T4, gp57A, which facilitates the formation of the long and short tail fibers, was isolated and characterized by peptide analysis, sedimentation equilibrium, and circular dichroism (CD). Sequence analysis confirmed the predicted sequence of 79 amino acids from the nucleotide sequence of the gene with the N-terminal methionine removed. The result led to the conclusion that the apparent smaller molecular weight of 6,000 from Tricine-sodium dodecyl sulfate-polyacrylamide gel electrophoresis than the expected molecular weight of 8,710 was due to its abnormal electrophoretic behavior instead of cleavage or processing of the gene product. Estimation of the secondary structure from far-UV CD indicated a 94% α-helix content, which was in accord with the prediction from the primary structure. A sedimentation equilibrium study, on the other hand, revealed that gp57A assumes a tetrameric subunit structure.

There are a number of T4 phage gene products on the assembly pathway of bacteriophage T4 that are essential for the phage growth but not incorporated in the mature virion. These include gp40, gp31, gp51, gp57A, gp38, and gp63 (gpX is the monomeric product of gene X). gp40 is essential for the formation of the initiation complex of the prohead (11); gp31 prevents abortive aggregation of the major head protein, gp23, and ensures the proper head shell formation (12); gp51 is necessary for the formation of the hub of the baseplate (21); gp57A facilitates the long and short tail fiber formation (2); gp38 is necessary for the formation of distal long tail fibers, functioning together with gp57A (24); and gp63 accelerates tail fiber attachment to the baseplate (25). Recently, gp31 was shown to function together with the *Escherichia coli* protein GroEL and can substitute for *E. coli* GroES (23). The exact mode of function of these proteins is not known, but they catalyze assembly reactions instead of constituting parts of the virion and thus are molecular chaperones.

In this study, we focused on gp57A, whose target proteins are concerned with the attachment of bacteriophage T4 to *E. coli*, i.e., the long tail fibers encoded by genes 34 through 37 (26) and the short tail fibers encoded by gene 12 (8, 14). The infection process starts when the free ends of the six long tail fibers, consisting of the C-terminal region of gp37, interact reversibly with the bacterial surface. Subsequently, the irreversible attachment of the phage occurs through the interaction between the short tail fibers and the host cell wall (19). The isolated trimeric gp12, P12, has been deduced to be a trimer based on its estimated diffusion coefficient, D_{20}, from gel filtration and its sedimentation coefficient, s_{20}, from density gradient ultracentrifugation (14). A recent study by scanning transmission electron microscopy (13) confirmed the trimeric subunit structure and reported the dimensions of the short tail fiber. P12 is 38 nm long and has an arrowhead-shaped head (10 nm long by 6 nm wide), which very likely corresponds to the C terminus of gp12 and will interact with the cell surface lipopolysaccharide, and has a 24-nm shaft of uniform width (3.8 nm) with a constricted center and a small tapered pin.

Herrmann and Wood (5) previously identified two proteins by sodium dodecyl sulfate-polyacrylamide gel electrophoresis (SDS-PAGE) as products of gene 57 with molecular weights of 6,000 (gp57A) and 18,000 (gp57B). They also showed that only gp57A is essential for growth of the phage. Subsequently, Herrmann (6) determined the nucleotide sequence of the gene 57 region and called one open reading frame gp57A. This was later shown by Broida and Abelson (1a) to be in the same open reading frame as gene 1. Broida and Abelson favored a different assignment of gene 57A, just downstream of gene 1, and predicted an 80-residue gene product despite the smaller molecular weight reported above. We demonstrate that the open reading frame as predicted by Broida and Abelson (1a) is indeed gene 57A by complete amino acid sequencing of gp57A and that it assumes a tetrameric subunit structure with a high α-helix content.

MATERIALS AND METHODS

Bacteria, plasmids, and bacteriophage. All strains, plasmids, and phage used in this work are listed in Table 1. Plasmid pTB5 contains gene 57A in pT7-5, which expresses genes under the T7 promoter (Fig. 1). The plasmid was transformed into *E. coli* BL21 (DE3), which carries T7 RNA polymerase on λDE3 integrated into the chromosome of BL21 (22).

Media, chemicals, and buffers. M9A medium and Luria broth (LB) were used to grow *E. coli*. M9A medium contained 6 g of Na_2HPO_4, 3 g of KH_2PO_4, 0.2 g of $MgSO_4 \cdot 7H_2O$, 0.5 g of NaCl, 1 g of NH_4Cl, 4 g of glucose, and 10 g of Casamino Acids (Difco Laboratories, Detroit, Mich.) per liter of water. LB medium contained 10 g of Bacto Tryptone, 5 g of yeast extract (Difco), and 10 g of NaCl per 1 liter of water. Buffer A and buffer B were used to purify gp57A. Buffer A contained, per liter, 12.11 g of Tris adjusted with HCl to pH 8.0. Buffer B contained, per liter, 1.21 g of Tris adjusted with HCl to pH 8.0 and supplemented with 0.1 M NaCl. Phage strains were stored in and diluted with phosphate buffer (PB^+), which contained 7 g of Na_2HPO_4 and 3 g of KH_2PO_4 per liter of water and which was supplemented with 1 mM $MgSO_4$.

In vivo complementation. *E. coli* BL21(DE3) cells with and without plasmid pTB5 were grown to a concentration of 4×10^8 cells/ml in M9A medium at 37°C with vigorous aeration. The burst sizes of the phage were 167, 3.3, and 0.05 PFU/cell for the induced cells, uninduced cells, and control (plasmidless) cells, respectively. Half of the cells from each culture were placed on ice (control and

* Corresponding author. Mailing address: Department of Life Science, Faculty of Bioscience and Biotechnology, Tokyo Institute of Technology, 4259 Nagatsuta, Midoriku, Yokohama 226, Japan. Phone: 81 45 924 5712. Fax: 81 45 924 5805. E-mail: farisaka@bio.titech.ac.jp.

TABLE 1. Bacterial strains, plasmids, and bacteriophage

Strain, plasmid, or phage	Relevant properties and use	Source or reference
E. coli strains		
BE	Su^-, nonpermissive for T4 ambers; selective plating and growth of am^+ phage	Our collection
B40(SuI)	Su^+; growth of T4 amber mutants	Our collection
BL21(DE3)	Carries T7 RNA polymerase on λDE3 integrated into the chromosome of BL21	Our collection; 22
Plasmids		
pT7-5	Expresses genes under T7 promoter, Ap^r	Our collection; 22
pTB5	Contains gene 57A in pT7-5	This work
Bacteriophage		
T4 57amE198	Gene 57A amber mutant	Our collection

uninduced cells). The remaining cultures were incubated with 0.1 mM isopropyl-β-D-thiogalactopyranoside (IPTG) for an additional 2 h at 37°C (induced cells). After induction, cells were recovered from culture by centrifugation at 5,000 × *g* for 5 min at 4°C and resuspended in the same volume of M9A medium. Cells were infected with T4 57am phage at a multiplicity of infection of 5, superinfected after an interval of 5 min, incubated for 2 h, and then chilled rapidly in an ice bath. After sedimentation of infected cells at 5,000 × *g* for 5 min at 4°C, the cells were resuspended in PB^+, and a few drops of $CHCl_3$ and 10 μg of DNase I (Sigma Chemical Co., St. Louis, Mo.) per ml were added to the mixture. The cell debris was removed from the suspension by centrifugation at 5,000 × *g* for 5 min at 4°C. The yield of T4 57am mutant phage was then measured on *E. coli* B40(SuI) to determine the in vivo complementation by gp57A.

Purification of gp57A. *E. coli* BL21(DE3)/pTB5 was grown at 37°C in 3 liters of LB medium with vigorous aeration to a concentration of 2×10^8 cells/ml. The cells were then induced with 0.5 mM IPTG and incubated for an additional 2 h. The induced cells were recovered from the culture by centrifugation at 10,000 × *g* for 30 min at 4°C. The pellet was resuspended in 30 ml of buffer A, homogenized by sonication for 15 min (10 pulses/s) in an ice bath, and centrifuged at 10,000 × *g* for 30 min at 4°C. The supernatant was loaded on a DEAE-Toyopearl column (TOSOH, Tokyo, Japan; 2.8 by 18.5 cm) which had been preequilibrated with the same buffer. The column was washed with 100 ml of buffer A, and the proteins were eluted with 400 ml of buffer A which contained a linear gradient of 0 to 0.5 M NaCl. gp57A is eluted at a concentration of 0.29 to 0.37 M NaCl. Fractions containing gp57A were collected, and ammonium sulfate was added to a final concentration of 2 M. The solution was then loaded on a phenyl-Toyopearl column (TOSOH; 2.8 by 18.5 cm) preequilibrated with buffer A with 2 M ammonium sulfate. The column was washed with 100 ml of the same buffer, and the proteins were eluted with 400 ml of the buffer with a reverse linear gradient of 2 to 0 M ammonium sulfate. gp57A is eluted at a concentration of 0.9 to 0.7 M ammonium sulfate. The fractions containing gp57A were collected and concentrated to a volume of 5 ml with an ultrafiltration cell with a YM3 membrane (Amicon, Beverly, Mass.) The concentrated gp57A was loaded on a Sephadex G-75 (Pharmacia LKB, Uppsala, Sweden; 2 by 100 cm) column preequilibrated with buffer B, and peak fractions containing gp57A were collected. The final yield of gp57A was 5.0 mg/10 g (wet weight) of cell. gp57A thus purified showed a single band on a Tricine-SDS-PAGE gel (18).

Gel electrophoresis and electroblotting. gp57A was run on a Tricine-SDS-PAGE gel containing 16.5% (wt/vol) acrylamide and stained with Coomassie brilliant blue G (Sigma) as described by Schagger and von Jagow (10, 18) after electrophoresis. gp57A was then electroblotted onto an Immobilon membrane (Millipore Corp., Bedford, Mass.), and the N-terminal sequence was determined by the method described below (7, 15).

Protein concentration determination. Protein concentration was routinely determined by the bicinchoninic acid (BCA) protein assay kit (Pierce, Rockford, Ill.) (20) with bovine serum albumin as a standard. When more accurate concentration was needed, as in the case of the circular dichroism (CD) measurements, the same solution that was used for the BCA protein assay was subjected to amino acid analysis and the absolute amount of Ala was used for correction. Concentration values obtained from the BCA method were thus corrected; the correction factor was determined to be 1.07.

N-terminal sequence analysis of gp57A. Automatic Edman degradation was carried out with a gas-phase sequencer (model 477A; Applied Biosystems, Foster City, Calif.). Phenylthiohydantoin derivatives of amino acids were analyzed with an on-line high-performance liquid chromatography (HPLC) system (Applied Biosystems model 120A).

Peptide mapping of gp57A by HPLC. Digestion with chymotrypsin (Sigma) was carried out at 37°C for 6 h in 0.1 M pyridine-collidine-acetate buffer (pH 8.2)–0.1 mM $CaCl_2$. The peptides in the digest were resolved in a reverse-phase HPLC (Waters 600 system), with a linear gradient of 0 to 80% acetonitrile in 0.1% trifluoroacetic acid (Pierce). An octyldecylsilane column (AP-302; YMC, Kyoto, Japan) (4.6 by 150 mm) was used. The elution profile was monitored by A_{215}.

Sedimentation equilibrium analysis. Sedimentation equilibrium analysis was carried out with an Optima XL-A analytical ultracentrifuge (Beckman, Fullerton, Calif.). Because gp57A does not possess any aromatic amino acids, the sedimentation equilibrium profile was monitored at 230 nm and the data were analyzed with XLAEQ software provided by Beckman. In the calculation of the molecular weight of gp57A, its partial specific volume was determined to be 0.71 from the concentration dependence of the density of gp57A solution at a number of concentrations from the formula $\rho = \rho_0 + (1 - \bar{v}\rho_0)c$, where ρ and ρ_0 are the observed densities of the gp57A solution and reference solution, respectively, $\bar{v}$ is

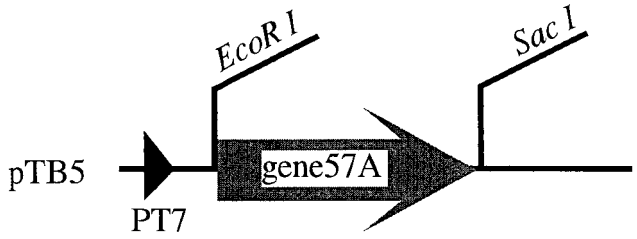

FIG. 1. Plasmid construction. Gene 57A was cloned in plasmid pT7-5 and designated pTB5.

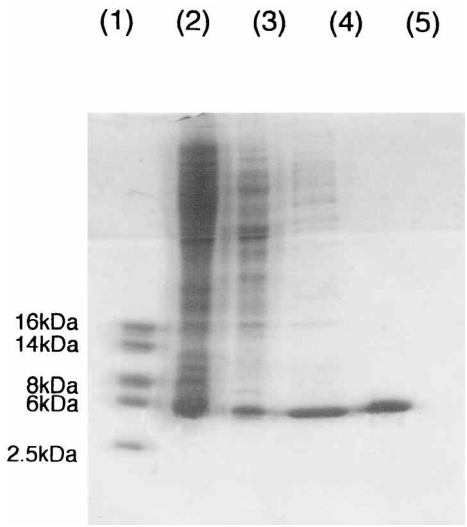

FIG. 2. Tricine-SDS-PAGE illustrating the purification of gp57A. Lanes: 1, molecular mass standard; 2, soluble fraction of cell extract of induced *E. coli* BL21(DE3)/pTB5; 3, gp57A containing fractions after DEAE-Toyopearl chromatography; 4, gp57A after phenyl-Toyopearl chromatography; 5, gp57A after Sephadex G-75 chromatography.

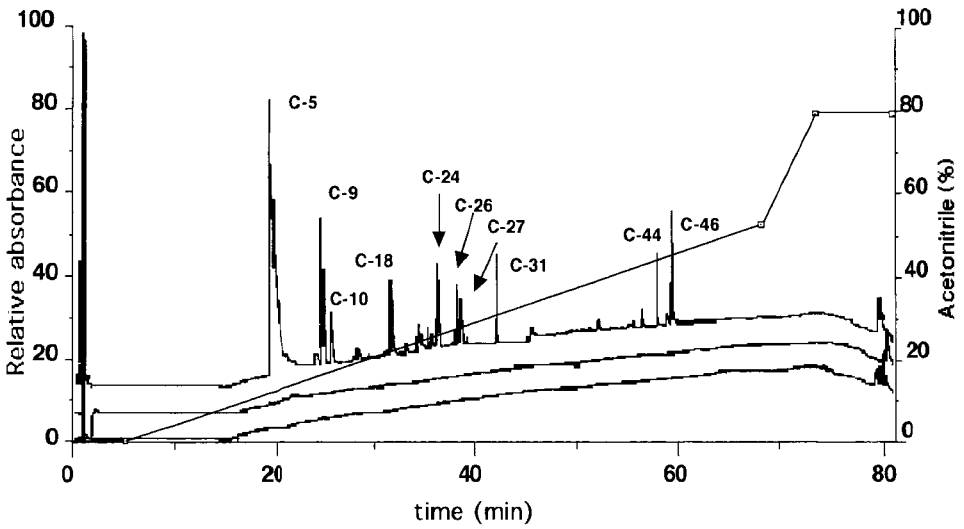

FIG. 3. Chromatogram of reverse-phase HPLC separation of chymotryptic fragments. The peptides in the digest were resolved in a reverse-phase HPLC (Waters 600 system) octyldecylsilane column (4.6 by 150 mm) with a linear gradient of 0 to 80% acetonitrile in 0.1% trifluoroacetic acid. The flow rate was 0.8 ml/min. The elution profile was monitored by A_{215}.

the partial specific volume of the protein, and c is the protein concentration (in grams per milliliter). The densities of gp57A solutions were measured with a DMA-58 density meter (Anton Paar, Graz, Austria).

CD and secondary structure estimation. The far-UV CD spectrum of gp57A between 190 and 240 nm was measured at 25°C on a J-500C spectropolarimeter (JASCO, Tokyo, Japan) in a 1-mm-path cell. This spectrum was used to estimate the secondary structure by CONTIN, a computer program developed by Steven W. Provencher (17).

Cross-linking of gp57A. Chemical cross-linking was carried out with 1.0% glutaraldehyde (BDH, Poole, England) at 25°C in 10 mM phosphate buffer (pH 7.6). The cross-linked gp57A was examined on a Tricine-SDS-PAGE gel (18).

RESULTS

As a first step towards elucidation of the mechanism of gp57A-assisted long and short tail fiber formation, we overexpressed gene 57A and purified and characterized the gene product.

Activity of gp57A in vivo. Prior to structural characterization of the gene product, the activity of the overexpressed gene product was examined by in vivo complementation as described in Materials and Methods. The in vivo complementation assay indicated that cloned and overexpressed gp57A complemented an amber mutant of T4 in gene 57A.

Purification of gp57A. After induction of gene 57A in *E. coli* BL21(DE3) by IPTG as described in Materials and Methods, gp57A was purified to homogeneity by three step column chromatographies; DEAE-Toyopearl chromatography, phenyl-Toyopearl chromatography, and Sephadex G-75 chromatography. The progress in purification with each step as monitored

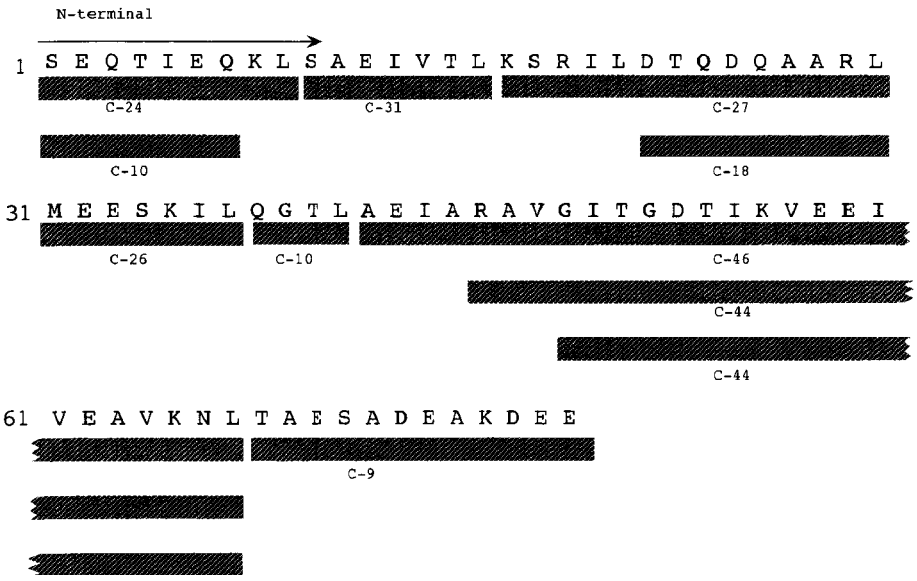

FIG. 4. Amino acid sequence of gene 57A product. The amino acid sequences of the purified chymotryptic peptides were analyzed by Edman degradation. The names of the peptides, shown beneath the sequences, correspond to the peptide peaks shown in Fig. 3. Edman degradation of the first 10 residues was also carried out on the complete gp57A protein indicated by an arrow at the N terminus.

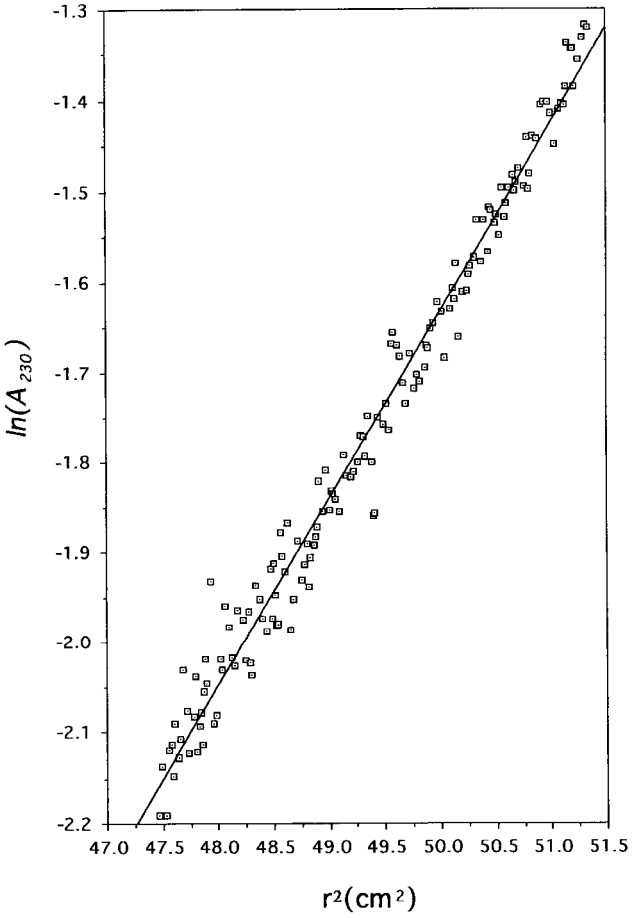

FIG. 5. Sedimentation equilibrium of gp57A. Because gp57A does not possess any aromatic amino acids, the concentration distribution was monitored at 230 nm. The profile suggests a homogeneous tetrameric subunit structure.

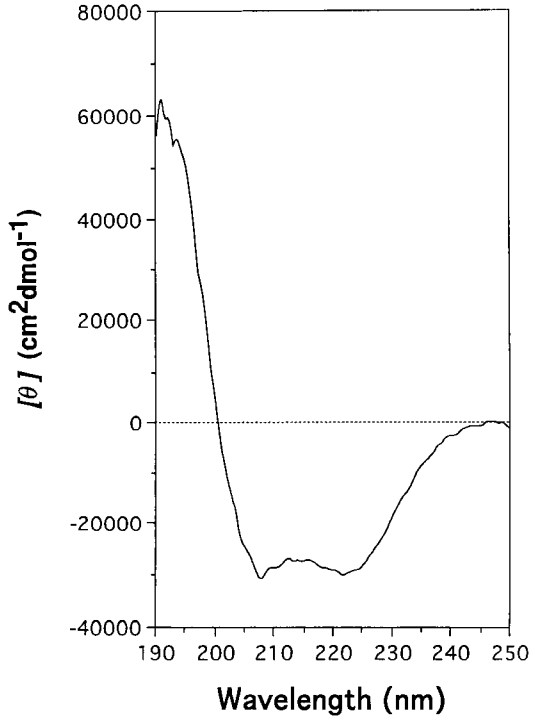

FIG. 6. Far-UV CD spectrum of gp57A. Estimation of the secondary structure as described by Provencher and Glockner gave a 94% α-helix content with no β-structure.

by Tricine-SDS-PAGE is shown in Fig. 2. The purified gp57A has a molecular weight of 6,000 estimated from Tricine-SDS-PAGE, which is in agreement with the finding of Herrmann and Wood (5) but about 30% smaller than the weight expected from the nucleotide sequence. Because of the significant difference, a possibility that processing of the polypeptide chain occurred was suspected.

Total amino acid sequence determination of gp57A. To confirm first that the overexpressed 6-kDa protein is in fact gp57A, we carried out amino-terminal sequence analysis by Edman degradation. The N-terminal sequence thus determined was identical to that deduced from the nucleotide sequence except that the N-terminal Met was removed and the fifth amino acid was Ile instead of Val as expected from the nucleotide sequence. It is not clear at present whether the discrepancy is due to the strain of the phage or a sequencing error of the nucleotide, but the two amino acids are similar in their physicochemical properties. We then proceeded to examine by peptide analysis the possibility that gp57A is processed in another part of the molecule. Chymotrypsin was used for a limited proteolysis, the major chymotryptic peptides were isolated by HPLC, and the amino acid sequences of the isolated peptides were determined. Figure 3 shows the separation of chymotryptic peptides of gp57A by HPLC. Figure 4 depicts the locations of the peptides for which Edman degradation was carried out. The determined sequences cover all of the primary structure predicted from the nucleotide sequence and thus confirm the amino acid sequence containing 79 amino acids. No processing of gp57A was observed. We conclude that the discrepancy between the apparent molecular weight from Tricine-SDS-PAGE and the molecular weight expected from the nucleotide sequence is due to an abnormal electrophoretic property of gp57A, although the physicochemical basis for the electrophoretic behavior remains to be explained.

Molecular weight determination of gp57A. To establish whether the native gp57A has a subunit structure, the molecular weight of gp57A in the active form was determined by sedimentation equilibrium centrifugation (Fig. 5). The molecular weight was estimated to be 33,470 ± 4,780 (mean ± standard deviation), indicating a tetrameric subunit structure. This value is close to 33,900, which is four times the molecular weight of a monomer, 8,481, estimated from the amino acid sequence. Chemical cross-linking of gp57A with glutaraldehyde supported the conclusion. Up to a tetrameric subunit structure of the cross-linked products was observed; no pentamer was detected (data not shown).

CD measurement and secondary structure prediction. The CD spectrum was measured in the far-UV region (Fig. 6), and the spectrum was analyzed by a program developed by Provencher and Glockner (17) to estimate the secondary structure of gp57A. The α-helical content was estimated to be 94% with no β-structure. The secondary structure prediction by the combined method of Nishikawa and Noguchi (16), based on the amino acid sequence, also gave a highly α-helical structure, i.e., 64% α-helix content with no β-structure (Fig. 7).

DISCUSSIONS

The concept of the mechanism of protein folding in the cell has changed over the past few years due to the discovery of

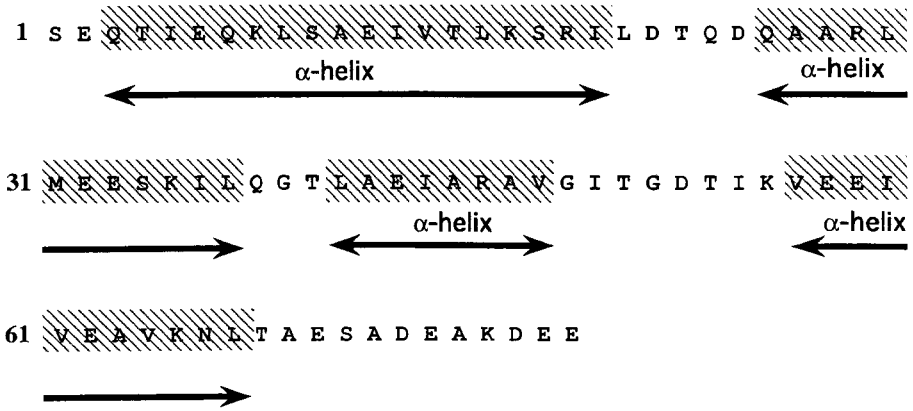

FIG. 7. Secondary structure prediction by the combined method of Nishikawa and Noguchi.

molecular chaperones (4). These are essential for the folding and/or assembly of many cellular proteins and are found ubiquitously in eubacteria, archaebacteria, and eucaryotes. Among them, the chaperonin GroEL of *E. coli* was originally found to be an essential host component for the growth of bacteriophage T4 and required for the assembly of the head (3). Phage T4 itself encodes several proteins which are essential for growth of the phage but not incorporated in the mature virion. We have focused on one such protein, gp57A, in the present study. gp57A catalyzes the formation of the long and short tail fibers, the former being encoded by genes 34 through 37 and the latter being encoded by gene 12 (8).

King and Laemmli (9) have previously shown that in the absence of gp57A, gp12 does not remain in the soluble fraction but instead is found in the cell debris or membrane fraction. On the basis of their observation, we isolated tails from T4 57Aam mutant phage lysates and confirmed that the tails do not possess gp12 (2a).

On the other hand, when gene 12 was overexpressed together with gene 57A, P12 is found associated with the membrane but is reversibly dissociated by treatment with EDTA (1). When gene 12 is expressed alone, the resultant gene product is associated with the membrane irreversibly and cannot dissociate with EDTA treatment. Also, the membrane-associated gp12 could be denatured by cold SDS. Taken together, these observations allow us to postulate that gp57A interacts with the nascent gp12 and facilitates formation of the native trimer, P12. Dissociation of P12 from the membrane, concomitant with its association with the baseplate, is one of the terminal steps in T4 morphogenesis.

The major aim of the present study has been to isolate and characterize gp57A as a first step towards understanding its function. The first problem we encountered was the discrepancy between the molecular weight from SDS-PAGE and that from the nucleotide sequence. We demonstrated that the primary structure is the same as that expected from the nucleotide sequence except that the N-terminal Met was removed and that the fifth residue was Ile instead of Val. From this result, it was concluded that the discrepancy in the molecular weight was due to the abnormal electrophoretic behavior instead of posttranslational processing.

The short tail fiber, P12, is a trimer at 37°C but tends to associate into a higher-molecular-weight aggregate at lower temperatures, e.g., at 20°C. The association is reversible. The dissociation of the higher-molecular-weight aggregate into trimers can be facilitated by the presence of gp57A (26a). The physiological significance of this function is not clear, but it may indicate an additional role of gp57A in facilitating the binding of P12 to the baseplate.

No significant homologies were detected in a search of the protein sequence database except for some α-helical proteins such as myosin and tropomyosin. In fact, gp57A is rich in α-helix as deduced from the CD spectrum (Fig. 6). Secondary structure prediction also supported the α-helix abundance in gp57A (Fig. 7). The native P57A is a tetramer of gp57A based on the molecular weight determination by sedimentation equilibrium (Fig. 5). The significance of the tetrameric subunit structure in relation to the function remains to be explained.

Efforts to crystallize gp57A for X-ray analysis are currently under way.

ACKNOWLEDGMENTS

We thank Takashi Kumazaki for valuable discussions and amino acid analysis, Ken Nishikawa for secondary structure prediction of gp57A, Yoshio Nishimura (Nihon Siber Hegner Co. Ltd.) for density measurements of gp57A solution, and Masaharu Kamo, Keiji Takamoto, and Norifumi Miyatake for advice concerning amino acid sequence analysis. We also thank A. Bokovsky and L. Grinius for their help and interest.

This work was supported in part by a grant to F.A. from the Ministry of Education, Science, and Culture of Japan. E.G. acknowledges financial assistance from the NSF (grant DCB-9006253).

REFERENCES

1. **Braun, R.** Personal communication.
1a. **Broida, J., and J. Abelson.** 1985. Sequence organization and control of transcription in the bacteriophage T4 tRNA region. J. Mol. Biol. **185:**545–563.
2. **Dickson, R. C.** 1973. Assembly of bacteriophage T4 tail fibers. IV. Subunit composition of tail fibers and fiber precursors. J. Mol. Biol. **79:**633–647.
2a. **Fukuda, E., and F. Arisaka.** Unpublished results.
3. **Georgopoulos, C. P., R. W. Hendrix, A. D. Kaiser, and W. B. Wood.** 1972. Role of the host cell in bacteriophage morphogenesis: effects of a bacterial mutation on T4 head assembly. Nature New Biol. **239:**38–41.
4. **Hendrick, J. P., and F. U. Hartl.** 1993. Molecular chaperone functions of heat-shock protein. Annu. Rev. Biochem. **62:**349–384.
5. **Herrmann, R., and W. B. Wood.** 1981. Assembly of bacteriophage T4 tail fibers: identification and characterization of the nonstructural protein gp57. Mol. Gen. Genet. **184:**125–132.
6. **Herrmann, R.** 1982. Nucleotide sequence of the bacteriophage T4 gene 57 and a deduced amino acid sequence. Nucleic Acids Res. **10:**1105–1112.
7. **Huang, J., and H. R. Matthews.** 1990. Application of sodium dodecyl sulfate-gel electrophoresis to low molecular weight polypeptides. Anal. Biochem. **188:**114–117.
8. **Kells, S. S., and R. Haselkorn.** 1974. Bacteriophage T4 short tail fibers are the product of gene 12. J. Mol. Biol. **83:**473–485.
9. **King, J., and U. K. Laemmli.** 1971. Polypeptides of the tail fibres of bacte-

riophage T4. J. Mol. Biol. **62:**465–477.
10. **Laemmli, U. K.** 1970. Cleavage of structural proteins during the assembly of the head of bacteriophage T4. Nature **227:**680–685.
11. **Laemmli, U. K., E. Molbert, M. Showe, and E. Kellenberger.** 1970. Form-determining function of the genes required for the assembly of the head of bacteriophage T4. J. Mol. Biol. **49:**99–113.
12. **Laemmli, U. K., F. Beguin, and K. G. Gujer.** 1970. A factor preventing the major head protein of bacteriophage T4 from random aggregation. J. Mol. Biol. **47:**69–85.
13. **Makhov, A. M., B. L. Trus, J. F. Conway, M. N. Simon, T. G. Zurabishvili, V. V. Mesyanzhinov, and A. C. Steven.** 1993. The short tail-fiber of bacteriophage T4: molecular structure and a mechanism for its conformational transition. Virology **194:**117–127.
14. **Mason, W. S., and R. Haselkorn.** 1972. Product of T4 gene 12. J. Mol. Biol. **66:**445–469.
15. **Matsudaira, P.** 1987. Sequence from picomole quantities of proteins electroblotted onto polyvinylidene difluoride membranes. J. Biol. Chem. **262:** 10035–10038.
16. **Nishikawa, K., and T. Noguchi.** 1991. Predicting protein secondary structure based on amino acid sequence. Methods Enzymol. **202:**31–44.
17. **Provencher, S. W., and J. Glockner.** 1981. Estimation of globular protein secondary structure from circular dichroism. Biochemistry **20:**33–37.
18. **Schagger, H., and G. von Jagow.** 1987. Tricine-sodium dodecyl sulfate-polyacrylamide gel electrophoresis for the separation of proteins in the range from 1 to 100 kDa. Anal. Biochem. **166:**368–379.
19. **Simon, L. D., and T. F. Anderson.** 1967. The infection of *Escherichia coli* by T2 and T4 bacteriophages as seen in the electron microscope. I. Attachment and penetration. Virology **32:**279–297.
20. **Smith, P. K., R. I. Krohn, G. T. Hermanson, A. K. Mallia, F. H. Gartner, M. D. Provenzano, E. K. Fujimoto, N. M. Goeke, B. J. Olson, and D. C. Klenk.** 1985. Measurement of protein using bicinchoninic acid. Anal. Biochem. **150:**76–85.
21. **Snustad, D. P.** 1968. Dominance interactions in *Escherichia coli* cells mixedly infected with bacteriophage T4D wild-type and amber mutants and their possible implications as to type of gene-product function: catalytic vs. stoichiometric. Virology **35:**550–563.
22. **Studier, F. W., and B. A. Moffatt.** 1986. Use of bacteriophage T7 RNA polymerase to direct selective high-level expression of cloned genes. J. Mol. Biol. **189:**113–130.
23. **van der Vies, S. M., A. A. Gatenby, and C. Georgopoulos.** 1994. Bacteriophage T4 encodes a co-chaperonin that can substitute for *Escherichia coli* GroES in protein folding. Nature **368:**654–656.
24. **Ward, S., and R. C. Dickson.** 1971. Assembly of bacteriophage T4 tail fibers. III. Genetic control of the major tail fiber polypeptides. J. Mol. Biol. **62:** 479–492.
25. **Wood, W. B., M. P. Conley, H. L. Lyle, and R. C. Dickson.** 1978. Attachment of tail fibers in bacteriophage T4 assembly. Purification, properties, and site of action of the accessory protein coded by gene 63. J. Biol. Chem. **253:** 2437–2445.
26. **Wood, W. B., F. A. Eiserling, and R. A. Crowther.** 1994. Long tail fibers: genes, proteins, structure, and assembly, p. 282–290. *In* J. D. Karam (ed.), Molecular biology of bacteriophage T4. American Society for Microbiology, Washington, D.C.
26a. **Yamazaki, K., T. Matsui, G. He, and F. Arisaka.** Unpublished data.